

Fusion and Plasma Physics Research at Los Alamos

Don Rej

36th Annual Meeting and Symposium

Fusion Power Associates

Washington, D.C.

December 15-16, 2015

Los Alamos Portfolio

Inertial Confinement Fusion

Magnetic Fusion Energy

High-Energy-Density Laboratory Plasmas

General Plasma Science

Work supported by:

NNSA (Science Campaigns, LDRD, NNSA Labs)

DOE Office of Science (FES, ASCR)

DOE ARPA-E

ITER Organization



Los Alamos Portfolio

Inertial Confinement Fusion

Magnetic Fusion Energy

High-Energy-Density Laboratory Plasmas

General Plasma Science

Work supported by:

NNSA (Science Campaigns, LDRD, NNSA Labs)

DOE Office of Science (FES, ASCR)

DOE ARPA-E

ITER Organization



LANL has completed the first series of ignition experiments with beryllium capsules

Scientific Achievement

LANL completed the first set of tuning experiments leading to the first DT layered implosion using a beryllium capsule. Data showed there is no significant impact on hohlraum energetics compared with CH capsules. Initial results show comparable performance to CH under similar conditions. This is consistent with the hypothesis that for high-foot, gas-filled hohlraums, the performance is dominated by drive asymmetry.

Significance and Impact

Higher Be ablation rate does not significantly impact hohlraum energetics making Be target designs viable

Implosion symmetry control in gas filled hohlraums challenging and believed to dominate performance (Clark et al.) which makes comparing ablator performance difficult

Research Details

With its low opacity and relatively high density, Be is believed to present a possibly more attractive, ablator material option

Future experiments will work towards a 1D like implosion platform to allow comparison of ablator performance

Ignition designs with Be capsules will use their higher efficiency to go to larger case-to-capsule ratios to improve implosion symmetry trading off x ray drive.

Key performance metrics for DT implosions

| Ablator | Be | CH |
|-------------------------------------|------------|------------|
| Shot | N150617 | N130501 |
| Power(TW) | 350 | 351 |
| Energy(MJ) | 1.41 | 1.27 |
| Y(13-15 MeV x 10 ¹⁴) | 7.8 ± 0.17 | 7.7 ± 0.16 |
| T _{ion} (keV) [#] | 3.65±0.13 | 2.96±0.13 |
| DSR(%) | 3.2±0.24 | 2.95±0.14 |
| Hot Spot Pressure (Gbar) | ~80 | 50-67 |

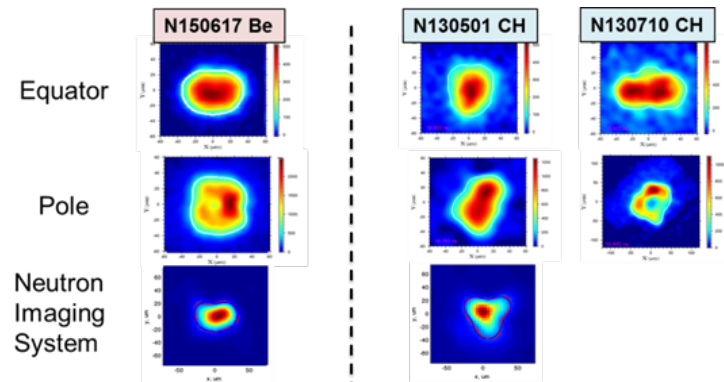
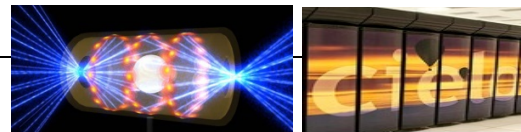


Table shows key performance metrics for first high foot Be capsule implosion with a companion CH shot. Lower figure shows implosion shape for first Be DT implosion for x ray self-emission with early CH DT implosions



Experiments show ablation front Rayleigh-Taylor growth in beryllium is less than predicted by simulations

Scientific Achievement

Using the hydro-growth radiography platform, seeded perturbations for a Beryllium capsule implosion were measured. The growth of these perturbations were less than predicted by simulations.

Significance and Impact

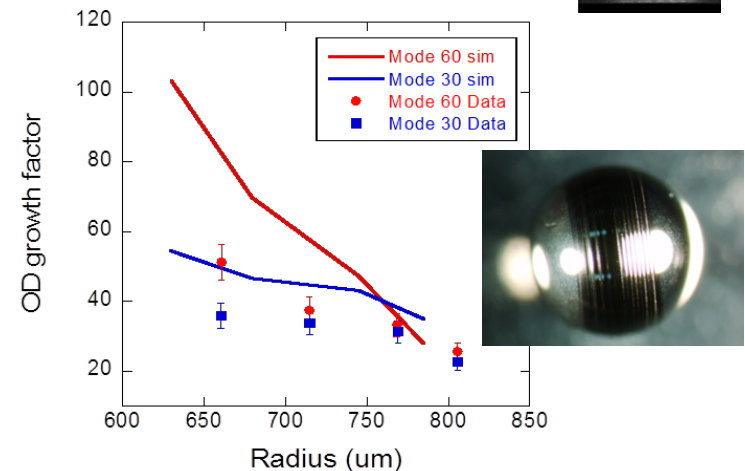
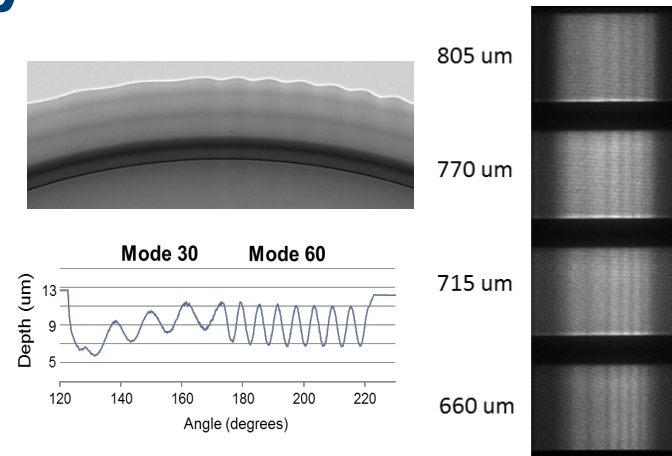
One advantage of beryllium is a higher ablation velocity which provide more stabilization to hydro-instabilities at the ablation front. This experiment is a confirms for ignition scale capsules. As a result, beryllium should be more robust to the tent (capsule mounting hardware) seeded instabilities currently thought to be a limiting factor for ICF implosions.

Research Details

The hydro-growth radiography platform uses machined perturbations to seed instabilities at the ablation surface of a capsule.

Growth of the perturbations are measured during an implosions using x-ray transmission measurements.

For beryllium, measurements of mode 30 and 60 show less growth than predicted by simulations for a high foot design.



Upper left: radiograph of initial perturbations in beryllium capsule with AFM trace.

Upper right: raw transmission data at different radii.

Lower: comparison of data with simulations for mode 30 and 60 with image of capsule

LANL is on track to test the first DT liquid layer, wetted foam target on NIF this month as a means to generate a 1D ignition implosion platform

Scientific Achievement

Target fabrication at LLNL has developed a method to add a thin, 50 μm thick, 35 mg/cc CH foam to the inside of a High Density Carbon (HDC) capsule. These capsules can be used to wick liquid DT into the foam to form a dense fuel layer for ignition implosions.

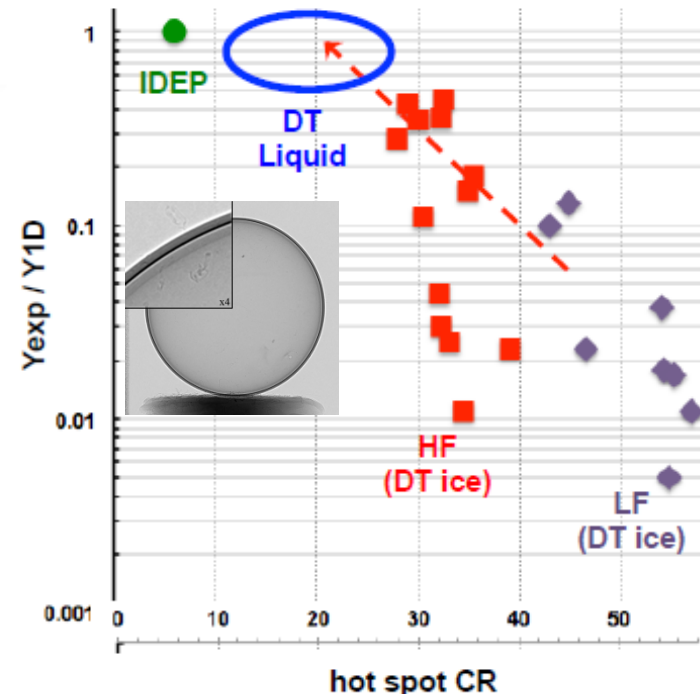
Significance and Impact

Unlike ignition capsules using DT ice layers which have to be fielded near the DT triple point, liquid layered capsules can be fielded over a range of temperatures. As the temperature is varied, the vapor pressure changes which changes the amount of initial residual gas in the hot spot. By varying the gas, the convergence of the implosion can be controlled while maintaining a dense DT fuel layer around the hot spot. Lower convergence implosions are expected to be more robust to 3D perturbations and perform more like a 1D implosion.

Research Details

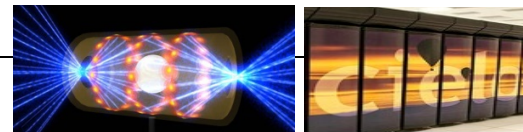
The first liquid layer capsule is scheduled for Dec. 20th. This shot will demonstrate the platform before executing a convergence scaling by varying the fielding temperature of the capsule.

Our hypothesis is that, without further reduction of 3D effects, experiments and 1D simulations will become similar at CR ~ 20 .



← Increased HS mass (Target fielding temp.)

Data showing implosion performance is more 1D like as hot spot convergence is reduced. Image of a foam filled HDC capsule is shown as an inset.



LANL is building two transformational diagnostics on NIF as part of the national diagnostics plan

Scientific Achievement

With an eye to the future, a long term national diagnostic plan has been developed for HED Science at the major NNSA facilities. At the top level are a set of transformational diagnostics expected to provide key measurements currently unattainable to test models. LANL is building on its work with gas Cherenkov detectors and Neutron imaging to generate such diagnostics.

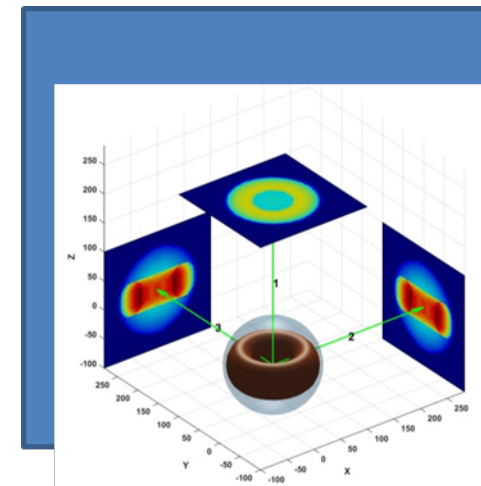
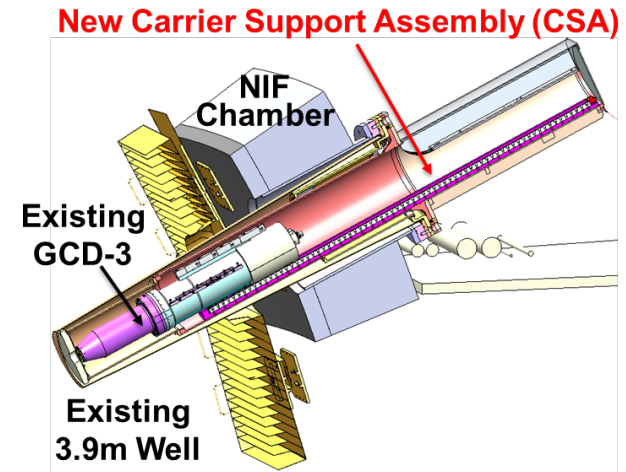
Significance and Impact

LANL is building the next generation gas Cherenkov detectors using faster photomultiplier tubes to increase temporal resolution from 100 ps down to ~20 ps. This will add 10x resolution elements over the burn of NIF ICF capsule. The detector will also be design for DIM carts to increase sensitive by 100x to gain dynamic range needed to see key failure signatures.

Additional neutron imagers are being added to provide images from different lines-of-sight. This will allow some rudimentary tomography and better comparisons with the multiple lines-of-sight for the x ray diagnostics

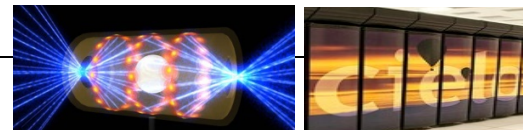
Research Details

Work on these diagnostics has begun and expected to be completed over the next couple years



Top: drawing of new gas Cherenkov detector insertion mechanism.

Bottom: Sample neutron imaging from 3 lines-of-sight for diagnosing 3D implosions



Los Alamos Portfolio

Inertial Confinement Fusion

Magnetic Fusion Energy

High-Energy-Density Laboratory Plasmas

General Plasma Science

Work supported by:

NNSA (Science Campaigns, LDRD, NNSA Labs)

DOE Office of Science (FES, ASCR)

DOE ARPA-E

ITER Organization



Operated by Los Alamos National Security, LLC for the U.S. Department of Energy's NNSA



W7-X First Operation

Scientific Achievement

After 19 years of construction, the W7-X stellarator began operations on December 10, 2015

Significance and Impact

The W7-X stellarator, a superconducting machine, with 10 MW of steady-state ECRH as its primary heating source, is designed to show that high performance DD plasmas can be operated for up to 30 minutes at a time. An extended startup involving 3 operating phases is planned for the next several years, slowly culminating with steady-state multi-keV DD plasmas.

Research Details

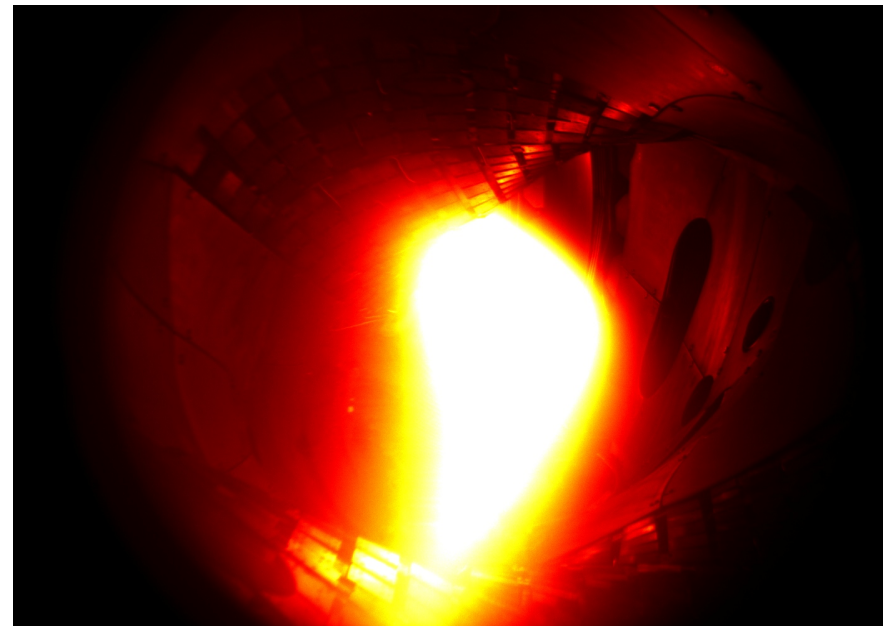
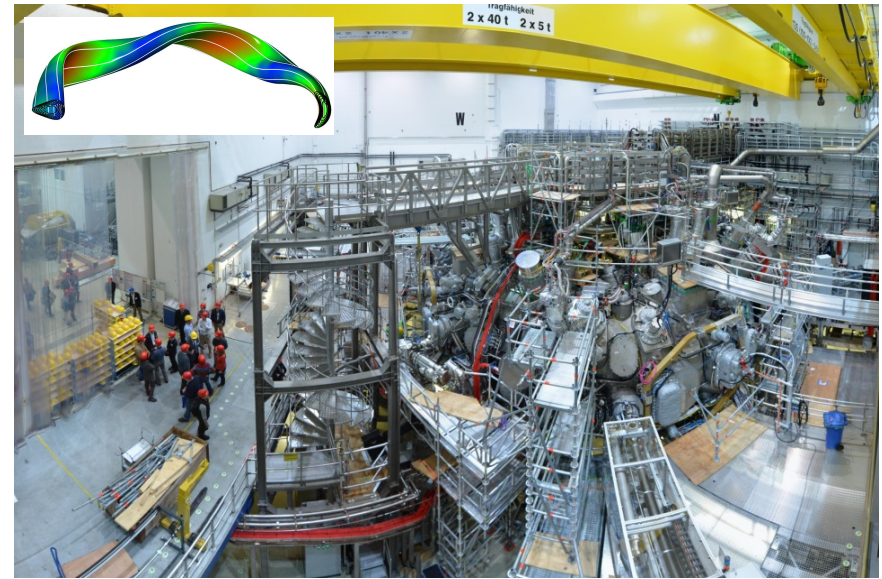
American diagnostics online for the first shots:

- Visible and infrared cameras viewing one of the limiters (LANL and Wisconsin)
- Visible filterscope array (ORNL and Wisconsin)
- Fast pressure gauges (Wisconsin)
- X-ray crystal spectrometer (PPPL began operations on Dec 11).

The use of the trim coils is not planned until Jan. 2016.

U.S. universities (MIT, U of Wisconsin, Auburn, and others) are now involved with next step diagnostics and modeling.

Ralf Koenig, J. Baldzuhn, W. Biel, C. Biedermann, H. S. Bosch, et al., "The Set of Diagnostics for the First Operation Campaign of the Wendelstein 7-X Stellarator", LA-UR-15-22439, 1st EPS Conference on Plasma Diagnostics, April 14-17, 2015, Frascati (Rome), Italy.



First plasma in Wendelstein 7-X on 12/10/15. It consisted of a helium at ~ 100 eV (colored black-and-white photo)

High-speed micropellets for magnetic fusion

Scientific Achievement

Potential applications for ELM pacing and stopping of energetic particles using high-speed micropellet injections in burning plasmas.

Significance and Impact

Intense heat and particle fluxes expected in ITER and beyond pose prohibitive problems to the design, selection and maintenance of the first wall and divertor materials.

Some innovative solutions to the material challenges may come from micropellet injection.

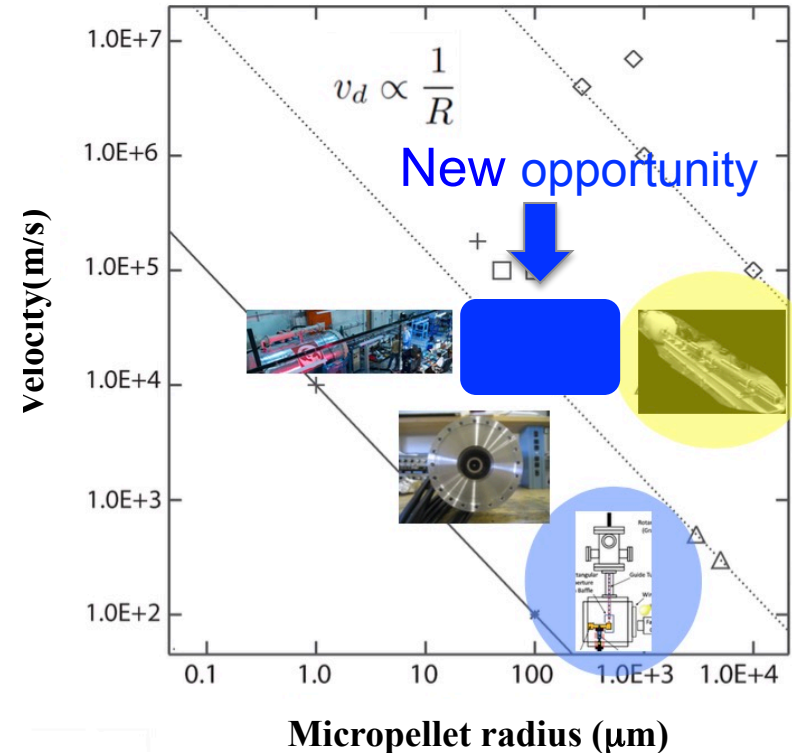
In addition to diagnostic applications, controlled injection of micropellets of different sizes and velocities at different frequencies will offer several possibilities:

- Better assessment of the core plasma cooling due to dust produced in-situ;
- Better understanding of the plasma-material interaction physics near the wall;
- New methods for plasma fueling and impurity control; and
- Reliable techniques that can achieve edge cooling without compromising the plasma core.

Research Details

Analytic models for micropellet-plasma interactions.

TRIM calculations for micropellet stopping of energetic particles.



A summary of various micropellet injection technologies. New opportunities exist for ~ 10 km/s, up to a few hundred micrometer size objects.

Work was led by Los Alamos National Laboratory.

Z. Wang, invited talk, 14th Workshop on the Physics of Dusty Plasmas, May 26-29 (2015); Z. Wang, R. Lunsford, D. K. Mansfield, J. H. Nichols, 'Existing and new applications of micropellet injection in magnetic fusion.' Manuscript submitted to IEEE Trans. Plasma Sci.

Under ARPA-E sponsorship, PLX- α aims to develop spherically imploding plasma liners formed by merging plasma jets as a versatile magneto-inertial-fusion driver*

Scientific Achievement

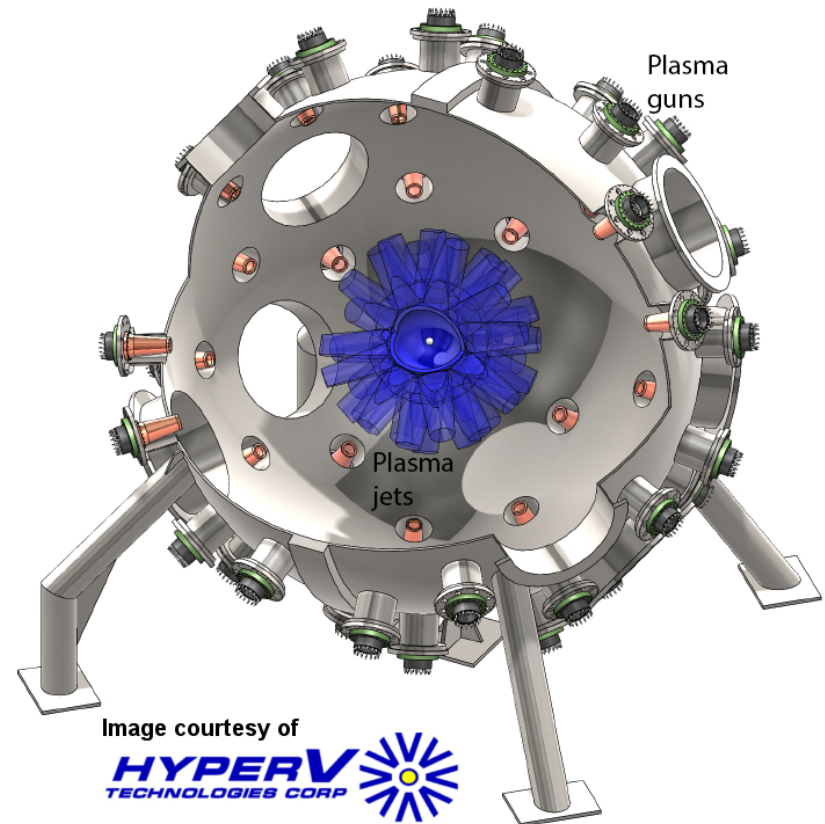
A series of analytic and computational papers has established the theoretical feasibility of forming spherically imploding plasma liners (via an array of merging supersonic plasma jets) as a versatile, standoff magneto-inertial-fusion driver. This, along with a demonstration of technological readiness of plasma-gun capabilities via focused single- and two-jet experiments, has led to an ARPA-E award for the experimental demonstration of plasma-liner formation.

Significance and Impact

If plasma liners can be formed with favorable ram-pressure and uniformity scalings (the key metrics for magnetized-target compression to fusion conditions), then they can enable a high-shot-rate and low-cost development path toward economical fusion power, which is the goal of ARPA-E's ALPHA program. Plasma liners have both high implosion velocity (to overcome target thermal transport rates) and standoff (allowing for high-shot-rate and low-cost R&D progress), making it unique among MIF drivers.

Research Details

The PLX- α project will demonstrate the viability and scalability of plasma liners as a standoff MIF driver, obtaining key data on liner ram-pressure and uniformity scalings, while benchmarking a suite of codes for designing potential future, scaled-up experiments.



C. Hsu et al., *IEEE Trans. Plasma Sci.* 40, 1287 (2012);
C. Hsu et al., *J. Plasma Physics* 81, 345810201 (2015).

Required budget of inner surface perturbations for efficient liner compression in magnetized target fusion

Scientific Achievement

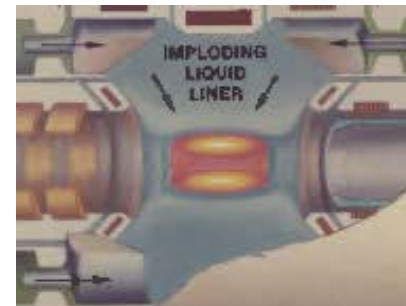
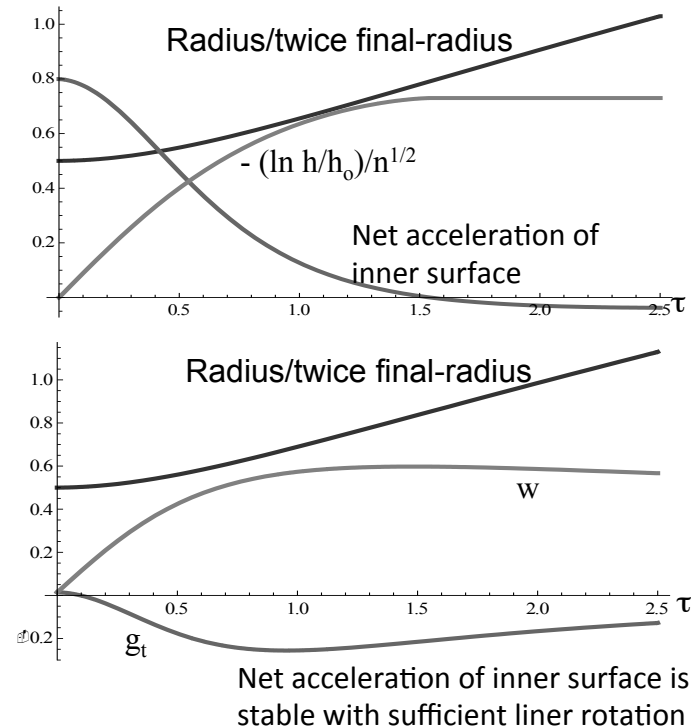
A dimensionless model for the final compression of a low density plasma/magnetic field target by an imploding cylindrical liner demonstrates the fundamental growth of perturbations due to Rayleigh-Taylor instability and provides a budget for initial amplitudes required for efficient energy transfer.

Significance and Impact

Corrects misimpression that faster liners can avoid such instability and recognizes stabilization based on liner rotation, which permits compact fusion reactor concepts.

Research Details

Analysis performs integration of perturbation growth for any mode number over unstable, final diameters of compression in normalized time and radius. Comparable results obtain for spherical liner implosion.



Stabilized Liner Compressor fusion reactor concept for ARPA-E ALPHA program by NumerEx LLC and NHMFL/LANL.



P.J. Turchi, "Liner Stability Problems for Megagauss Fusion," *IEEE Trans. on Plasma Science*, 43, 1, Part II, 369 (2015).

UNCLASSIFIED

NumerEx, LLC



arpa-e
CHANGING WHAT'S POSSIBLE



Sheath Energy Transmission

Scientific Achievement

First-principle simulation and theoretical model for sheath energy transmission.

Significance and Impact

Sheath energy transmission underpins plasma-materials interaction in a tokamak reactor.

Research details:

Found supersonic instead of sonic exit flow → much larger ion sheath energy transmission coefficient.

Electron sheath energy transmission has a significant component due to correlation between perpendicular and parallel degrees of freedom.

$$\begin{aligned}\gamma_e^{se} &= (1 + \alpha) \frac{q_{e,n}^{se}}{\Gamma_{e\parallel}^{se} k_B T_{e\parallel}^{se}} + \frac{3}{2} + \frac{T_{e\perp}^{se}}{T_{e\parallel}^{se}} \\ &= (1 + \alpha) \left(-\frac{e\Delta\Phi^{sh}}{k_B T_{e\parallel}^{se}} + \frac{T_{e\parallel}^0}{T_{e\parallel}^{se}} - \frac{3}{2} \right) + \frac{3}{2} + \frac{T_{e\perp}^{se}}{T_{e\parallel}^{se}}.\end{aligned}$$

Tang & Guo, PoP, 2015

TABLE I. Simulation results for $m_i/m_e = 1600$. Here, $\alpha \equiv 2q_{e,s}^{se}/q_{e,n}^{se}$ and $\gamma_e^{se(-)} \equiv \gamma_e^{se} - q_{e,s}^{se}/\Gamma_{e\parallel}^{se} k_B T_{e\parallel}^{se}$. The γ_e^{se} and γ_i^{se} are computed from the simulated Q_{\parallel}^{se} and $\Gamma_{\parallel} T_{\parallel}^{se}$.

| $\frac{\lambda_{mfp}}{\lambda_{de}}$ | M | $\frac{T_{i\parallel}^{se}}{T_{e\parallel}^{se}}$ | $\frac{T_{i\perp}^{se}}{T_{i\parallel}^{se}}$ | $\frac{T_{e\perp}^{se}}{T_{e\parallel}^{se}}$ | $\frac{e\Delta\Phi^{sh}}{k_B T_{e\parallel}^{se}}$ | γ_i^{se} | γ_e^{se} | $\gamma_e^{se(-)}$ | α |
|--------------------------------------|------|---|---|---|--|-----------------|-----------------|--------------------|----------|
| 5 | 1.31 | 1.34 | 1.04 | 1.00 | -1.82 | 5.86 | 3.86 | 3.33 | 0.64 |
| 16.7 | 1.23 | 1.38 | 1.09 | 1.01 | -2.02 | 5.60 | 4.24 | 3.58 | 0.61 |
| 50 | 1.16 | 1.35 | 1.31 | 1.05 | -2.16 | 5.42 | 4.85 | 4.22 | 0.38 |
| 166.7 | 1.08 | 1.18 | 2.03 | 1.09 | -2.30 | 5.95 | 5.27 | 4.70 | 0.27 |

TABLE II. Model predictions for $m_i/m_e = 1600$. The four dimensionless input parameters of the model, M , $T_{i\parallel}^{se}/T_{e\parallel}^{se}$, $T_{i\perp}^{se}/T_{i\parallel}^{se}$, and $T_{e\perp}^{se}/T_{e\parallel}^{se}$, are taken from the simulation data tabulated in Table I.

| $\frac{\lambda_{mfp}}{\lambda_{de}}$ | $\Delta\varphi^{sh}$ | $\frac{T_{e\parallel}^{se}}{T_{e\parallel}^0}$ | $\frac{e\Delta\Phi^{sh}}{k_B T_{e\parallel}^{se}}$ | γ_i^{se} | γ_e^{se} |
|--------------------------------------|----------------------|--|--|-----------------|-----------------|
| 5 | -1.79 | 0.87 | -2.07 | 5.75 | 4.23 |
| 16.7 | -1.84 | 0.87 | -2.11 | 5.41 | 4.27 |
| 50 | -1.90 | 0.88 | -2.17 | 5.33 | 4.36 |
| 166.7 | -2.02 | 0.89 | -2.27 | 5.77 | 4.49 |

$$\gamma_i^{se} \equiv \frac{Q_{i\parallel}^{se}}{\Gamma_i^{se} k_B T_{i\parallel}^{se}} \approx \frac{1}{2} M^2 \left(3 + \frac{T_{e\parallel}^{se}}{T_{i\parallel}^{se}} \right) + \frac{3}{2} + \frac{T_{i\perp}^{se}}{T_{i\parallel}^{se}}$$

Dust charging at dust size \sim Debye length regime

Scientific achievement:

Develop dust charging theory for tokamak regime of dust size \sim Debye length.

Significance and impact:

Accurate prediction of dust charge is essential for understanding dust transport and survivability in a tokamak.

Research detail:

Known Orbital-Motion-Limited OML theory *can not predict dust charge* in any regime (Allen, et al, 2000), past usage relies on Whipple (1981) approximation (invoking standard Debye shielding to relate dust potential and charge).

Revised OML (Tang & Delzanno, PoP, 2014) corrected an error in OML ion density expression, can now predict dust charge by solving OML Poisson equation.

Validates the Whipple approximation in zero dust size limit,

Demonstrates good agreement with full PIC result in dust size/Debye length ~ 1 regime – fusion relevant.

(Delzanno & Tang, PoP, 2015)

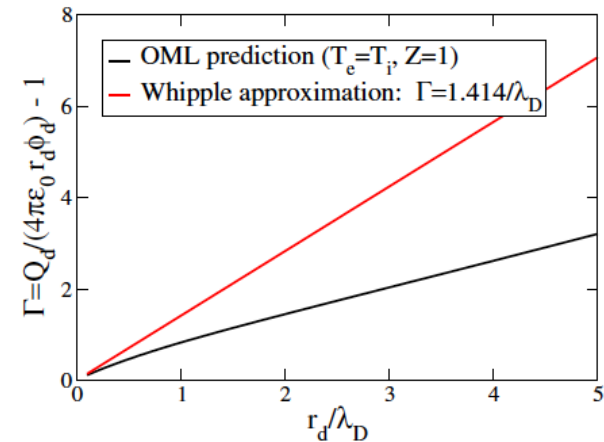
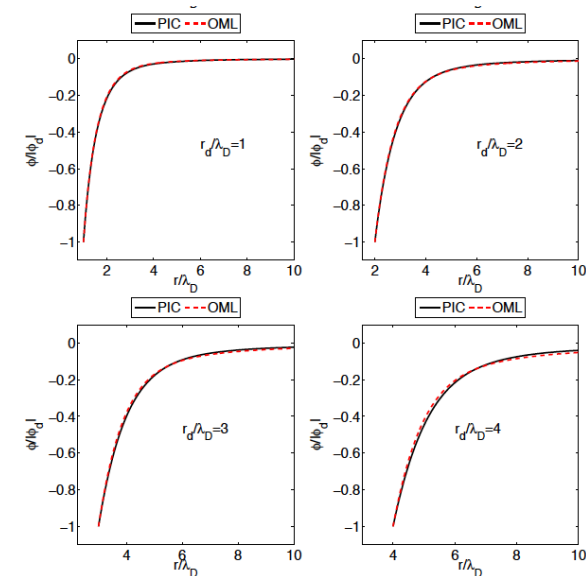


FIG. 4. Dust capacitance is shown as a function of r_d/λ_D . The deviation from Eq. (38) becomes large when the dust size becomes comparable or greater than the Debye length.



Torques due to error fields locking to finite plasma velocity

Scientific Achievement

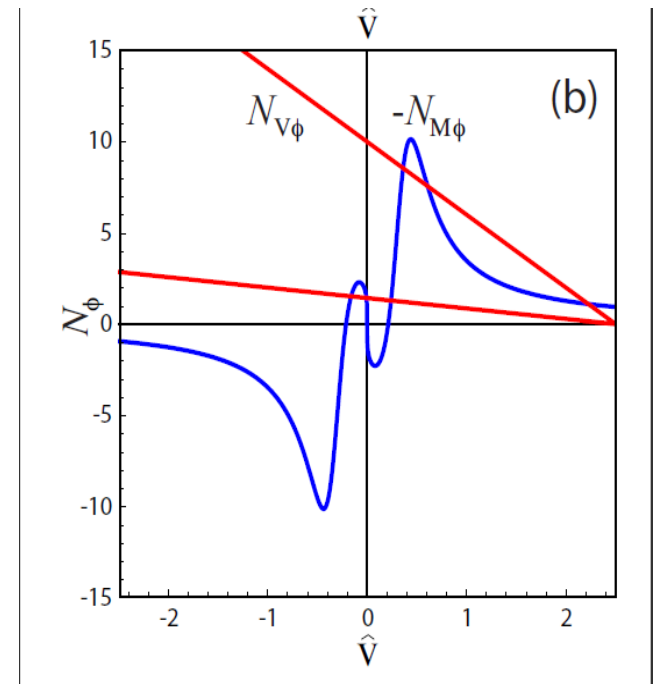
Discovered that the response of a tearing layer to an external field and the torque of the layer is distinctly different for layers with a finite frequency response.

Significance and Impact

For tearing modes with finite real frequencies – e.g. Glasser effect – the mode response to an error field is largest when the plasma velocity equals the phase velocity of the tearing mode. The torque due to the error field locks the plasma to this velocity, and this could prevent disruptions.

Research Details

This basic effect has escaped notice for decades. The maximum response is for rotation such that the phase velocity of the backward wave in the lab frame is zero. The torque applied at the tearing layer is peaked just to the right of the phase velocity of the mode (plasma frame), so that the plasma will lock to this velocity. This observation leads to the possibility of driving significant flow in plasmas such as ITER, and rotation shear can be generated by driving at several rational surfaces.



Streamfunction contours: The torque as a function of the plasma rotation rate. This torque is zero at the phase velocity, leading to a locked mode with *nonzero* plasma velocity. Depending on the other parameters of the system, the unlocked state and an unstable intermediate state can occur.

Momentum Transport due to Error Fields

Scientific Achievement

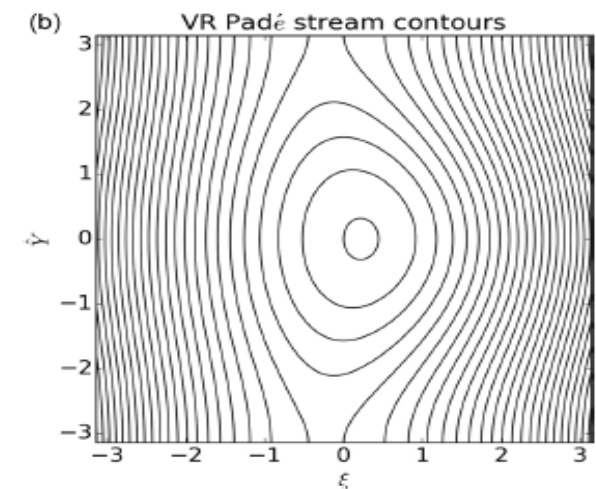
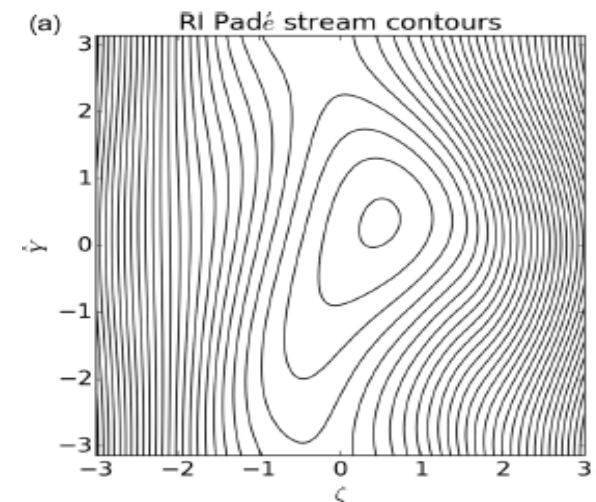
Calculated the forces on tearing layers due to externally driven magnetic fields. Calculated the moments across the tearing layers and related them to the effects driving zonal flows.

Significance and Impact

Forces on tearing layers can lock plasma to an error field or to other MHD modes, which often leads to disruptions. In the presence of rotation shear, the Reynolds moment can decrease the rotation shear across the tearing layer, affecting the stability and the likelihood of disruptions.

Research Details

A known expression for the Maxwell force on a tearing layer was shown to have the same form with rotation shear. The Reynolds force was shown to exist be be smaller. The Maxwell moment across the layer was shown to be small. The Reynolds moment was shown to be small and zero for viscoresistive tearing modes, but important for the resistive-inertial mode. This moment is similar to the moment that drives zonal flows.



Streamfunction contours: (Upper panel) Streamfunction contours for resistive-inertial layers; (Lower panel) Streamfunction for viscoresistive layers. The symmetry in the latter case leads to zero Reynolds moment.

Near-surface He bubble growth and bursting in tungsten at irradiation rates appropriate for fusion-plasma conditions

Scientific Achievement

Accelerated molecular dynamics simulation of He bubble growth and bursting in tungsten at rates of relevance to reactor operation.

Significance and Impact

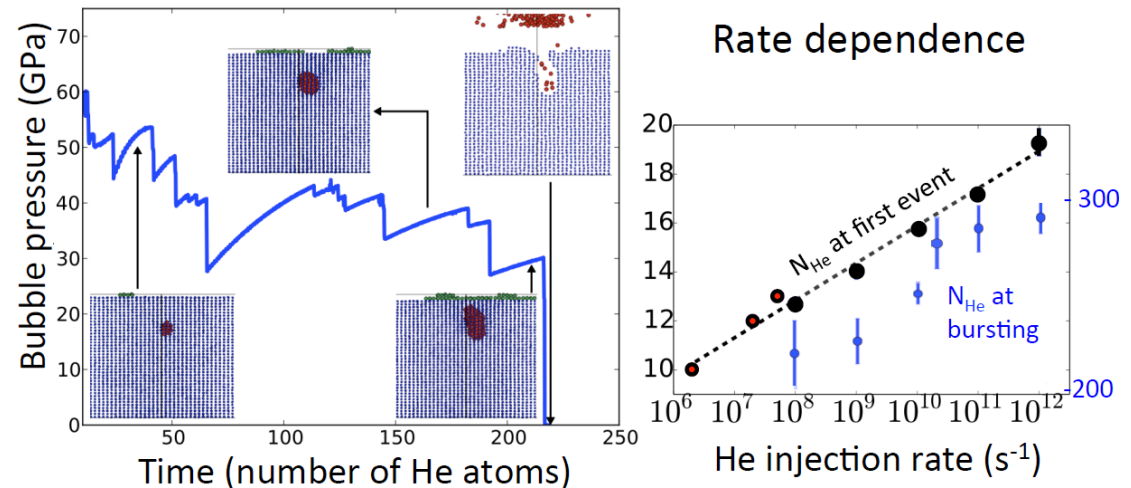
First simulation of He bubble growth at He irradiation flux appropriate for fusion first-wall in ITER. The simulations find a qualitatively different growth mode when rates approach experimental values. They reveal rate effects on bubble size, shape, pressure, and surface damage.

Research Details

Parallel Replica Dynamics simulations of bubble growth with He injection rate ranging from 10^{12} s^{-1} to $2 \times 10^6 \text{ s}^{-1}$. Efficient to petascale: utilized 160,000 cores (over half of Titan) at ORNL at 77% efficiency.

Slower growth leads to smaller, more anisotropic bubble that grows in a directed way towards surface, producing fewer adatoms during growth and creating less surface damage upon bursting.

Collaboration with BES program Accelerated Molecular Dynamics (Voter) at LANL



Left: Growth/bursting at intermediate (near-crossover) rate (10^9 He/s). Helium pressure is relieved via emission of W interstitials. At slower growth rates, interstitials have time to diffuse over surface of bubble, ultimately emitting more interstitials from top in the form of dislocation loops (crowdion clusters) that travel to surface, leaving adatoms.

Right: Dependence of bubble properties on bubble growth rate.

L. Sandoval, D. Perez, B.P. Uberuaga, and A.F. Voter;
Physical Review Letters, in press. Work performed at LANL,
computing at ORNL.

Effect of Damaging Temperature on Deuterium Retention in Tungsten

Scientific Achievement

Ion irradiation damage performed under elevated temperatures are found to allow defects/traps to recover and thus to reduce overall deuterium retention in tungsten.

Significance and Impact

Established fusion plasma relevant temperature condition for first wall material to be simulated with ion irradiations in lieu of neutron damage.

Research Details

Well-polished W coupons were irradiated with 5-MeV Cu ions at LANL-IBML to a variety of fluences under different temperatures (up to 1243 K).

Irradiated W specimens were exposed at UCSD-PIECES by 100 eV D ions to 10^{24} D/m² at 383 K.

Exposed W specimens were analyzed for D-profile at LANL-IBML by nuclear reaction analysis.

The specimens were back to UCSD-PIECES and analyzed for total D content by thermal desorption spectroscopy.

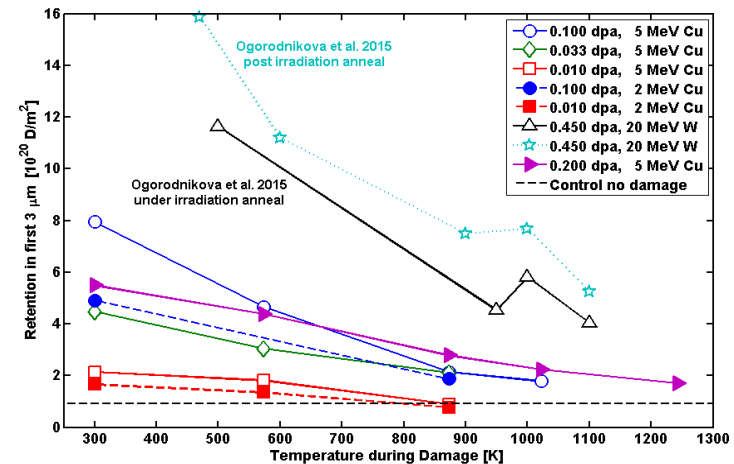
M. Simmonds, Y.Q. Wang, R.P. Doerner, J.L. Barton, M.J. Baldwin, G.R. Tynan, presented at 15th International Conference on Plasma Facing Materials and Components, Aix en Provence, France, May 18-22, 2015.



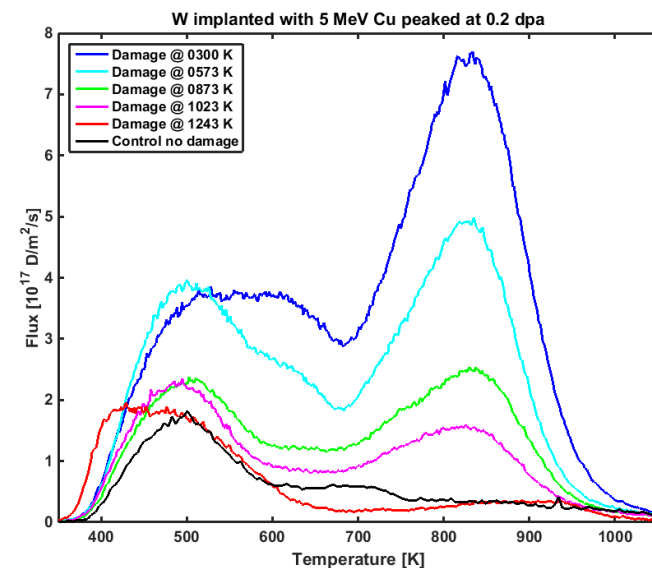
UNCLASSIFIED

Operated by Los Alamos National Security, LLC for the U.S. Department of Energy's NNSA

D-retention is decreased by ~70% at Divertor relevant temperatures



Thermal Desorption Spectroscopy data suggest three types of defect traps for deuterium atoms in W



Nanomechanical Properties of Single- and Dual-Beam Damaged Tungsten

Scientific Achievement

He ions are found to play a dominant role in controlling hardening and yield strength as compared with W ions.

W (111) and (110) grains are found to be harder than W (100) grains, but the irradiation induced hardening is very similar in all three types of grains.

Significance and Impact

Established spherical nanoindentation technique to probe nanomechanical properties of single and dual-beam damaged tungsten.

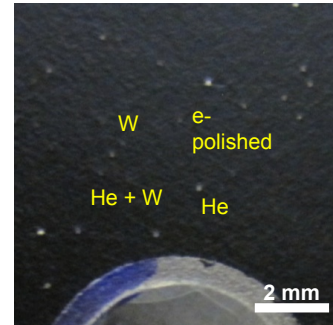
Research Details

Well-polished W coupons were irradiated with multiple energies of W and He ions to achieve flat damage profiles.

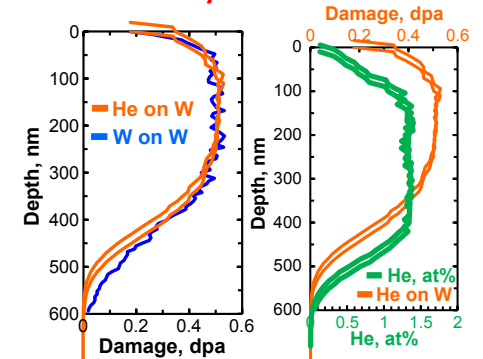
He ion damaged region showed significant hardening and increased yield strength as compared to that W ion damaged region with the same calculated dpa.

Observed hardening effect in W is almost independent of irradiation temperature (RT – 500 C) and irradiation dose (0.2 – 2 dpa) used.

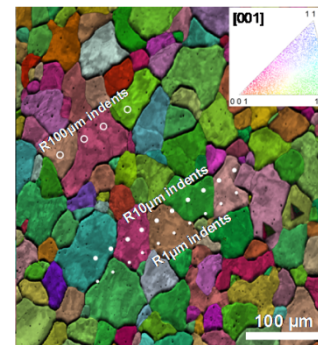
W implanted/irradiated with He, W, and He+ W beams



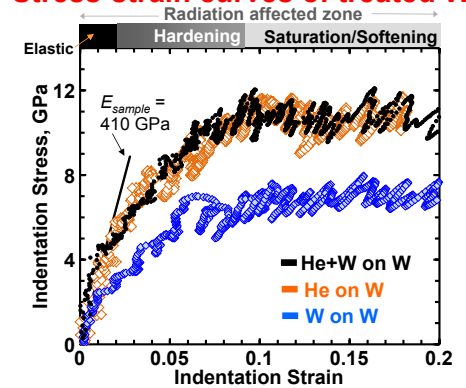
Damage and helium depth profiles in W by Monte Carlo



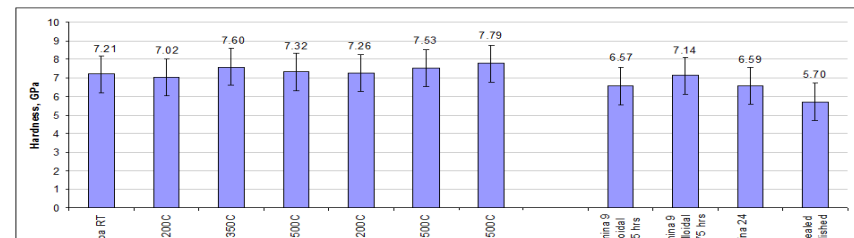
W-grain size and orientation



Stress-strain curves of treated W



Irradiation dose and temperature effect on W-hardness



Tritium Fuel Cycle Research

Scientific Achievement

LANL Chemical Diagnosis and Engineering Group has developed a hydrogen processing laboratory (HPL) capability to act as a surrogate for tritium fuel cycle research and development. The capability continues to support FES and ITER projects

Significance and Impact

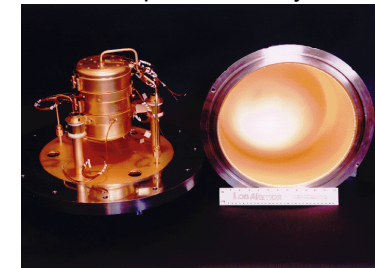
The HPL capability can support all aspects of a tritium fuel cycle such as impurity separation, isotope separation, and storage and delivery systems designs. The use of hydrogen as a surrogate allows process verification without the added cost/risk associated with a nuclear facility.

Current Research Details

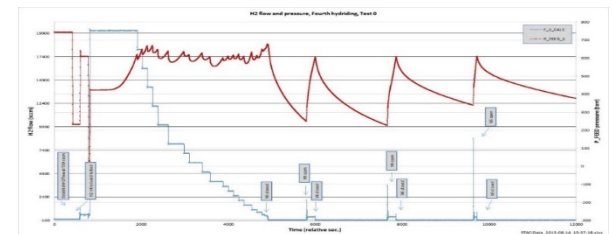
- **STACI U-bed unit has completed four hydride/dehydride experiments**
 - Have identified multiple areas to increase performance and are implementing upgrades to STACI design for continued testing
- **Tritium Processing Export Control Guidance Whitepaper**
- **Continuing to plan TSTA data-mining project.**



STACI Hydride/Dehydride Experimental System



Self-assaying Tritium Accountability and Containment unit for ITER (STACI)



Experimental data from STACI Hydrating Run

Los Alamos Portfolio

Inertial Confinement Fusion

Magnetic Fusion Energy

High-Energy-Density Laboratory Plasmas

General Plasma Science

Work supported by:

NNSA (Science Campaigns, LDRD, NNSA Labs)

DOE Office of Science (FES, ASCR)

DOE ARPA-E

ITER Organization



Laboratory investigation of magnetized collisionless shocks

Scientific Achievement

MSX is the first experiment to achieve plasma flows that are:

- magnetized w/ roughly equal magnetic and thermal energies,
- collisionless over shock length and time scales,
- supersonic (w.r.t. fast magnetosonic speed) & supercritical,
- and with shock length & timescales small enough to fit within the experiment but large enough to observe w/ available diagnostics.

Significance and Impact

Magnetized, collisionless, supercritical shocks are by far the most common type of shock in the universe. They are thought to play a large role in the overall partition of energy throughout the cosmos by generating non-thermal ion and electron distributions, producing turbulence and instabilities that give rise to extreme density and magnetic field perturbations, and accelerating particles to relativistic cosmic-ray energies.

Research Details

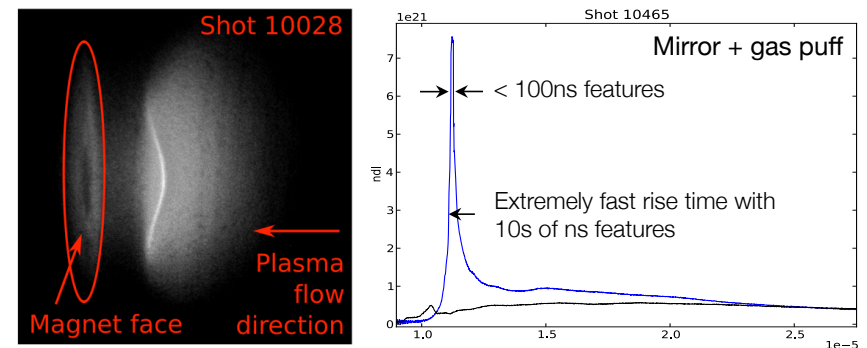
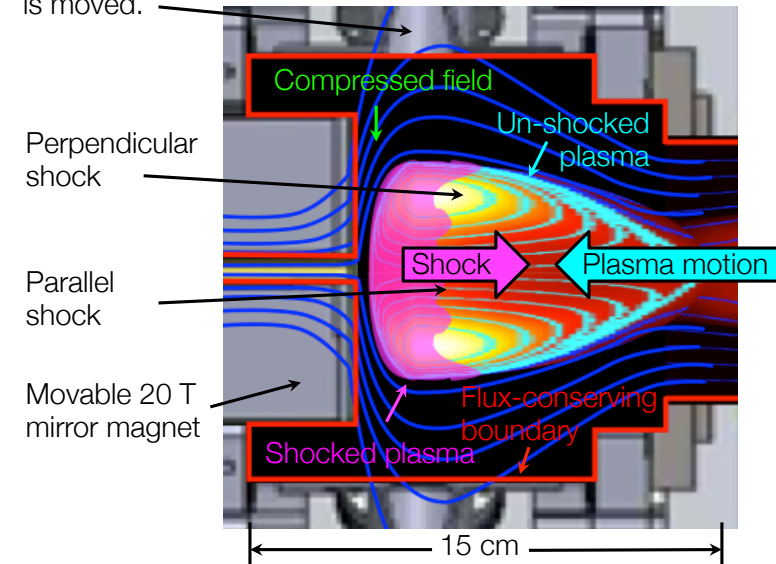
- MSX generates magnetized, collisionless, supercritical flows that stagnate against a variety of “pistons”:
- Magnetic mirror and/or flux-conserving boundary
- Cusp (supersonic reconnection)
- Neutral gas puff (w. or w.o. magnetic field)
- Novel optical distributed magnetic diagnostics being developed in collaboration with the U.Washington.

T.E. Weber, T.P. Intrator, R.J. Smith, *Rev. Sci. Instr.*, 85, 043501 (2014).

T.E. Weber, T.P. Intrator, R.J. Smith, *Phys. Plasmas*, 22, 042518 (2015).

Work performed at Los Alamos National Laboratory

Diagnostic ports allow scanning across plasma when magnet is moved.



Examples of plasma stagnation: (left) visible light framing image, (right) chord-averaged density.

UNIVERSITY OF WASHINGTON

Los Alamos NATIONAL LABORATORY EST. 1943



U.S. DEPARTMENT OF ENERGY

Office of Science



Observation of Rayleigh-Taylor-instability evolution in a plasma with magnetic and viscous effects

Scientific Achievement

Head-on-merging plasma jets (of an argon/impurity or hydrogen/impurity mixture) in the presence of an applied magnetic field (Fig. 1) have provided detailed data on Rayleigh-Taylor-instability (RTI) evolution relevant for astrophysical and imploding-fusion problems.

Significance and Impact

Our best computer codes cannot yet accurately predict detailed RTI growth and evolution in the presence of magnetic and viscous effects, even though this is an important problem for astrophysics and fusion (e.g., during deceleration-phase instability of the pusher/target interface in magneto-inertial fusion or magnetized ICF).

Research Details

Detailed diagnostic data, including CCD images (Fig. 2), interferometry, spectroscopy, and Bdot measurements, and comparisons with idealized 2D MHD simulations, were used to show consistency of the observations with RTI modified by magnetic and/or viscous effects.

C. S. Adams, A. L. Moser, and S. C. Hsu, *Phys. Rev. E* **92**, 051101(R) (2015); invited talk at 2015 APS-DPP.

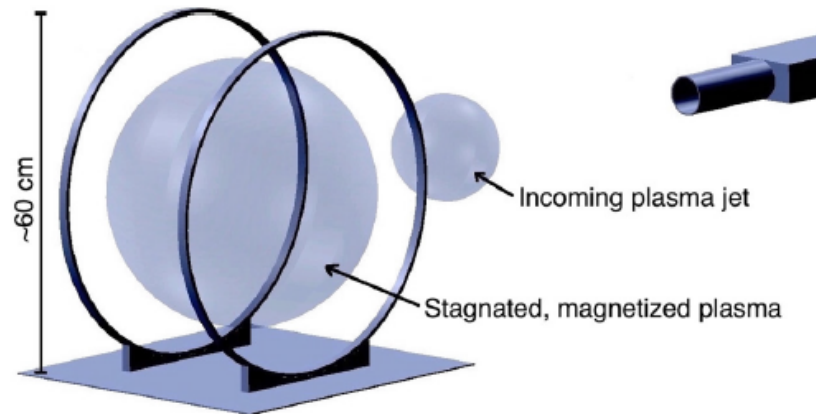


Fig. 1: Experimental setup: two plasma jets launched by oppositely positioned railguns (only one shown at right) collide head-on near the center of an in-chamber Helmholtz coil, giving rise to stagnated, magnetized plasma. The interaction of a second jet (formed due to the ringing railgun current) colliding with the stagnated plasma is studied in detail using a suite of diagnostics, as indicated in Fig. 2.

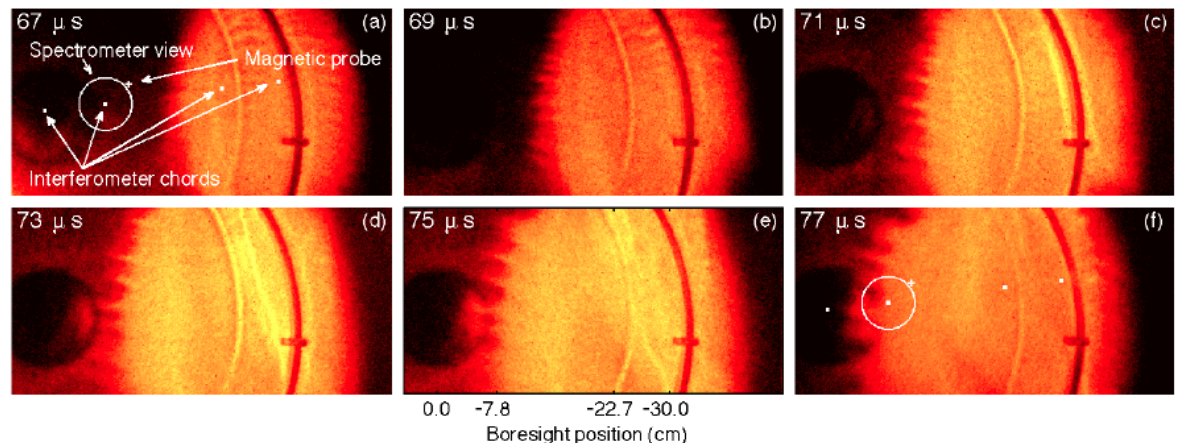


Fig. 2: Fast-camera images (from a single shot) of a plasma jet (bright region, incoming from right) colliding with a stagnated plasma (dark region, left) embedded within an applied magnetic field (portions of in-chamber Helmholtz coils are visible). Fingers evolve toward longer wavelengths at the decelerating interface, consistent with Rayleigh-Taylor-instability evolution in the presence of magnetic and/or viscous stabilization.

UNCLASSIFIED

Exploring the Theoretical Similarities between Quark-Gluon Plasmas and Warm Dense Matter

Scientific Achievements

We constructed a predictive theory, the effective potential theory, that extends traditional (Landau-Spitzer) plasma transport theory to the strongly coupled regime (see Fig. 1) and is in agreement with recent experimental measurements (see Fig. 2).

We applied the analytically derived stopping power dE/dx for heavy quarks (fermions) in a strongly interacting plasma to predict the suppression of photon-tagged b-jets at the Large Hadron Collider (LHC) (See Fig. 3)

Significance and Impact

Our project advances the understanding of strongly coupled plasmas in the coupling regime the $\Gamma \sim \text{few}$. Wide range of applications – from imploding ICF capsules to the core of Jovian planets and quark-gluon plasmas (QGPs).

Research Approach

We employ state-of-the-art analytic and numerical simulation techniques to describe the plasma response, energy loss, and the modification of the jet cross sections in the plasma

S.D. Baalrud and J. Daligault, Phys. Rev. E 91, 063107 (2015); , AIP Conf. Proc. 1168, 04002 (2015);
Invited talk at Int. Conf. on Non-Neutral Plasmas, Japan (Dec. 2014);

J. Huang, Z. Kang, I. Vitev, Phys. Lett. B750 (2015) 287-293;

Z. Kang, R. Lashof-Regas, G. Ovanesyan, P. Saad, I. Vitev, Phys. Rev. Lett. 114 (2015) 9, 092002



UNCLASSIFIED

Operated by Los Alamos National Security, LLC for the U.S. DEPARTMENT OF ENERGY



U.S. DEPARTMENT OF ENERGY

Office of Science

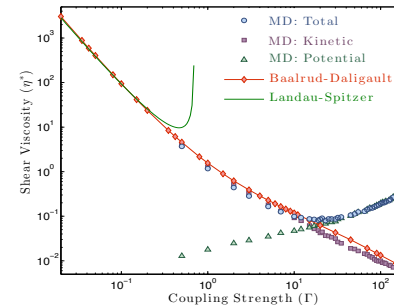


Figure 1. Comparison of the MD results for the shear viscosity coefficient with the Landau-Spitzer prediction, and the effective potential theory of Baalrud-Daligault.

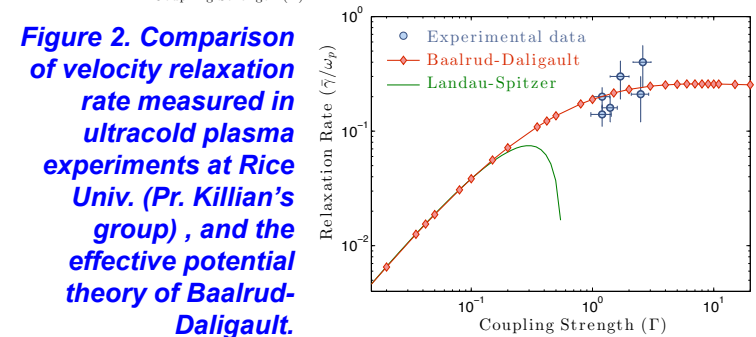


Figure 2. Comparison of velocity relaxation rate measured in ultracold plasma experiments at Rice Univ. (Pr. Killian's group), and the effective potential theory of Baalrud-Daligault.

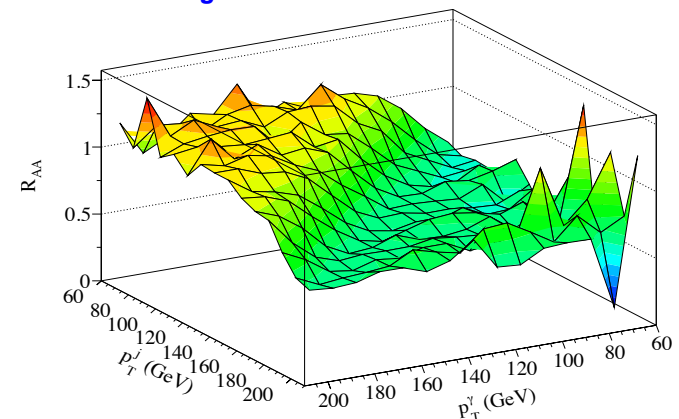


Figure 3. Prediction for the modification of the cross section for photon-tagged jets in Pb+Pb heavy ion reactions at the LHC. The collisional stopping power dE/dx of strongly interacting plasmas is applied on the developing quark-gluon shower.

Fast and accurate quantum molecular dynamics of dense plasmas across temperature regimes

Scientific Achievement

We have developed a new simulation method that allows accurate ab-initio simulations of dense plasmas spanning from low temperature (e.g., liquid metal) to high temperature (e.g., inertial confinement fusion plasma) conditions. The new method is significantly less computationally expensive (Fig.1) and provides the same accuracy as the established approaches (Figs 2,3).

Significance and Impact

A significant challenge of high energy density physics (HEDP) is the determination of the fundamental properties of plasmas (e.g., equation of state, transport properties). Accurate and wide ranging simulations of such plasmas have up to now been severely restricted due to the enormous computational expense of established ab-initio methods. Our method allows for a self-consistent determination of equation-of-state and transport properties of HEDP systems over much broader temperature and density regimes than previously accessible.

Research Details

Our novel fast and accurate quantum molecular dynamics method was used to determine self-consistently the thermodynamic and transport properties of dense plasmas relevant to current HEDP experiments.

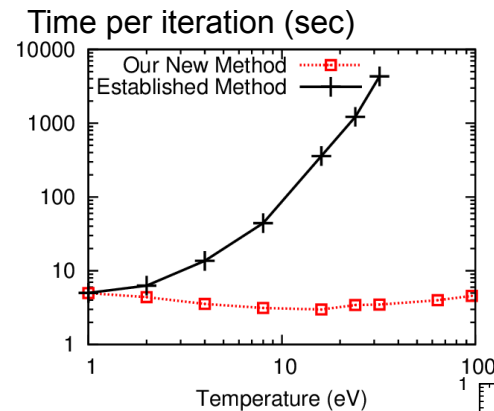


Fig. 1: Prohibitive temperature scaling of established methods (a.k.a. Kohn-Sham DFT) is shown, whereas our method extends to all temperatures without increased cost.

Fig. 2: Shear-viscosity coefficient of Deuterium plasmas from cold to hot conditions

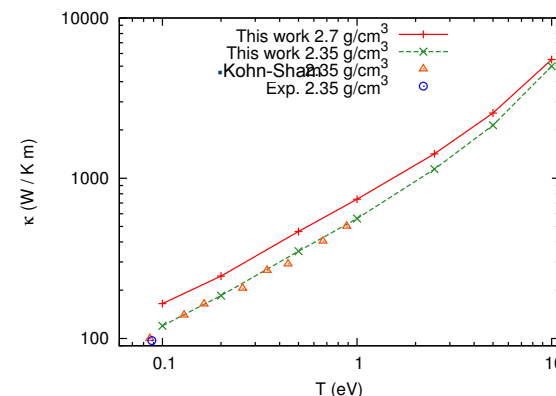
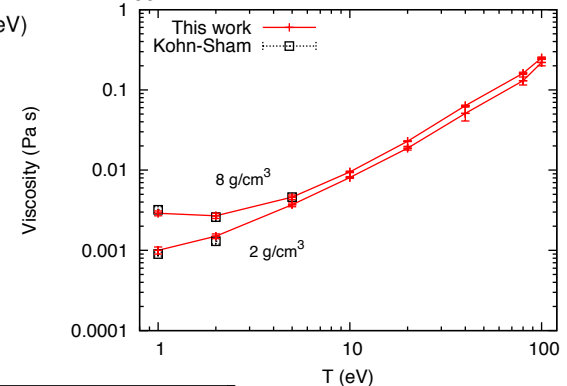


Fig. 3: Electronic thermal conductivity of warm dense Aluminum plasmas

Los Alamos Portfolio

Inertial Confinement Fusion

Magnetic Fusion Energy

High-Energy-Density Laboratory Plasmas

General Plasma Science

Work supported by:

NNSA (Science Campaigns, LDRD, NNSA Labs)

DOE Office of Science (FES, ASCR)

DOE ARPA-E

ITER Organization



Pulsating Magnetic Reconnection Driven by 3D Flux-Rope Interactions

Scientific Achievement

Plasma physicists at UCLA and LANL have measured the 3D dynamics of magnetic reconnection in a laboratory experiment with two interacting flux ropes.

Significance and Impact

Flux ropes are ubiquitous magnetic structures in astrophysical plasmas, and their interaction can give to magnetic reconnection. In this study, field-line mapping diagnostics were employed to precisely characterize the 3D reconnection dynamics and energy conversion.

Research Details

Experiment employed two 7.5 cm diameter flux ropes, 11m long

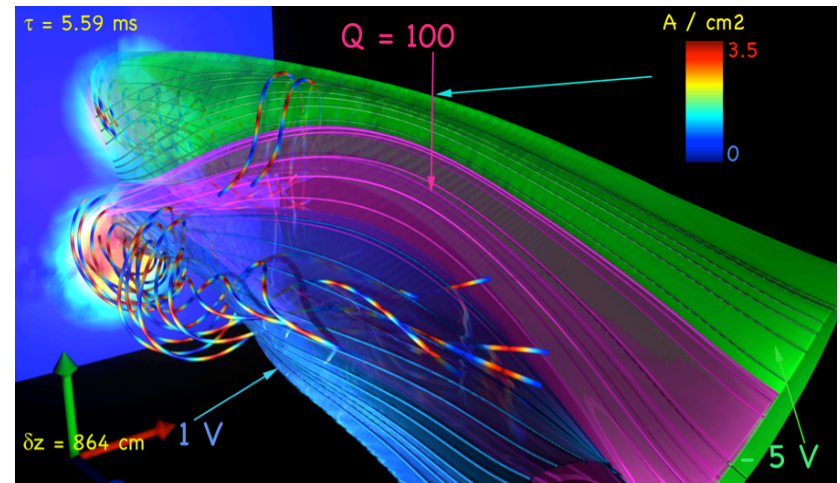
Electric and magnetic fields measured at 42k positions

Squashing factor Q computed - gives separation rate of B-lines

Quasi-potential computed by integrating E_{\parallel} along B-lines

Quantified non-linear reconnection, which pulsates in time

Electron pressure gradient and resistivity balance E_{\parallel} in the Quasi-Separatrix Layer (QSL)



UCLA Flux-Rope: Quasi-separatrix layer with $Q=100$ is shown in magenta during a flux rope collision at $t = 5.5856$ ms. Diverging magnetic field lines within the QSL are visible. Also shown are two isosurfaces of the quasi-potential, computed by integrating the parallel electric field along magnetic field lines. The maximum value of the quasi-potential is directly related to the nonlinear reconnection rate.

W. Gekelman, T. DeHaas, W. Daughton, B. Van Compernelle, T. Intrator, S. Vincena. Submitted to *Phys. Rev Let.* 2015



Particle Energization in Magnetically Dominated Plasmas

Scientific Achievement

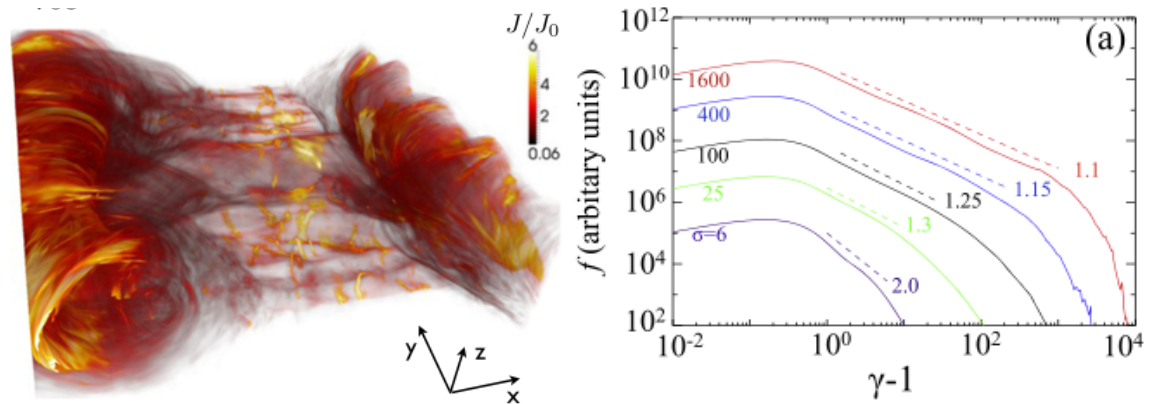
We have performed extensive Particle-In-Cell studies of particle acceleration associated with magnetic reconnection in the low beta limit. We found that significant non-thermal particle distributions can be produced. We further analyzed the mechanisms that are responsible for the power-law, which is related to a Fermi-like acceleration process by curvature drifts.

Significance and Impact

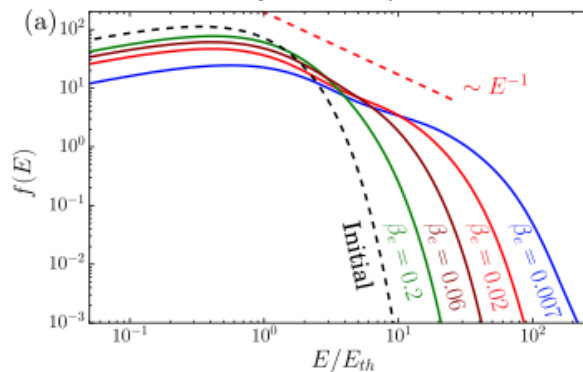
These simulations were the first in producing power-law non-thermal particle distributions from reconnection process. This result can be applied to observations in solar flares, jets from black holes and gamma-ray bursts.

Research Details

Large-scale 2D and 3D particle-in-cell simulations were performed using a force-free equilibrium with low beta or magnetic energy density exceeding the rest mass energy density of the plasmas. Detailed analyses using particle tracing reveal that Fermi-like acceleration mechanism is important. Plasma turbulence is observed as well.



Dynamics of 3D relativistic collisionless reconnection with current ropes and filaments (left) and the associated relativistic particle energy distribution (right).^{1,2} As the amount of magnetic energy increases, the accelerated particle distributions get harder (right). Such highly non-thermal particle distributions are needed to explain several high energy astrophysical observations in jets from black holes and gamma-ray bursts.



Particle energy distributions from a magnetically dominated but non-relativistic collisionless reconnection, showing the production (for the first time) of the power-law distribution.³ The existence of the power-laws critically depends on the plasma beta. This result can be applied to the particle acceleration as observed in solar flares.

Work supported by DOE FES

¹ Guo, F., Liu, Y-H., Daughton, W., Li, H., "Particle Acceleration and Plasma Dynamics during Magnetic Reconnection in the Magnetically Dominated Regime", ApJ, 806, 167 (2015)

² Guo, F., Li, H., Daughton, W., Liu, Y-H., "Formation of Hard Power Laws in the Energetic Particle Spectra Resulting from Relativistic Magnetic Reconnection", PRL, 113, 155005(2014)

³ Li, X., Guo, F., Li, H., Li, G. "Nonthermally Dominated Electron Acceleration during Magnetic Reconnection in a Low-beta Plasma", ApJ Letters, 811, L24 (2015)

Fast Magnetic Reconnection with Large Guide Fields

Scientific Achievement

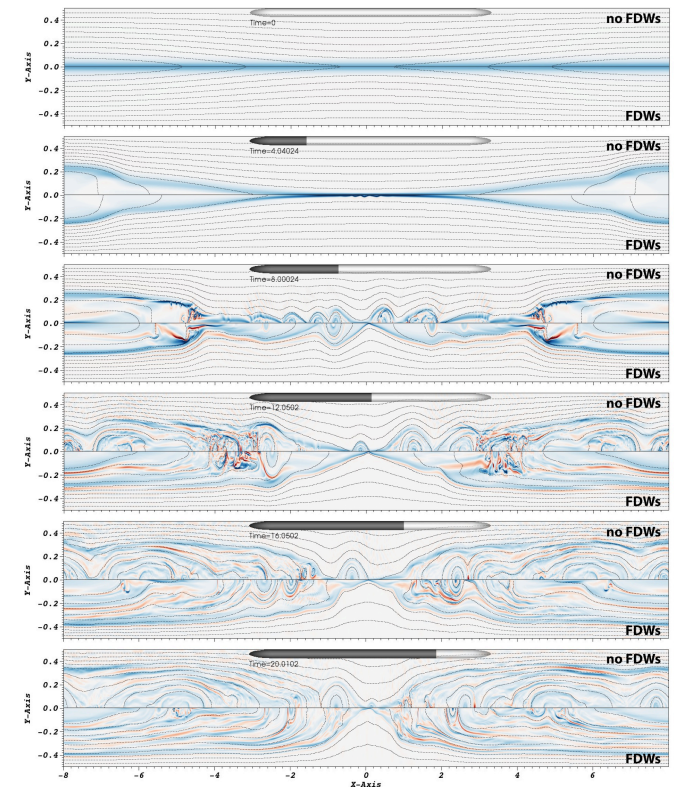
In this work it has been demonstrated that two-fluid magnetic reconnection with strong guide field is fast, independent of dissipation and system size, regardless of the presence of fast-dispersive waves. A discrete model was constructed that predicts how the diffusion region must self-adjust such that the rate of reconnection is dissipation independent. These predictions are verified by fluid simulations, and give good agreement with fully kinetic results for the large scale evolution.

Significance and Impact

To explain many magnetized plasma phenomena, it is crucial to understand how the rates of magnetic reconnection scale in large and weakly collisional systems. These results have important implications for understanding reconnection in the solar corona, and in laboratory magnetic confinement devices. Furthermore, it is demonstrated that the two fluid model is sufficient to model large scale evolution in these environments at a much reduced computational cost when compared with fully kinetic simulations.

Research Details

The reconnection rate is determined by the outer diffusion region of thickness $h = \max(\rho_s, d_e)$, where ρ_s is the sound Larmor radius and d_e the electron skin depth. These are the scales at which electron diamagnetic effects and electron inertia become important respectively.



Plasma current profiles (color scale) and magnetic fluxes (contours) from fluid (PIXIE2D) simulations for Harris-sheet reconnection problem without fast-dispersive waves (FDWs, top half of each panel) and with fast dispersive waves (no FDWs, bottom halves).

Work performed at Los Alamos National Laboratory.

Fusion Rockets for Planetary Defense

Scientific Achievement

A new idea has been proposed, to use fast fusion-driven rockets with a large nuclear explosive payload, to be able to intercept and defect long-period comet threats to the Earth.

Significance and Impact

Only fusion rockets have the combination of specific power and high exhaust velocity needed to put an interceptor rocket out to Jupiter distances in 3-6 months. The problem with comets falling in from the Oort Cloud, is that they arrive with little warning, and are first visible only as they begin to warm up at Jupiter to Saturn distances (5-10 AU).

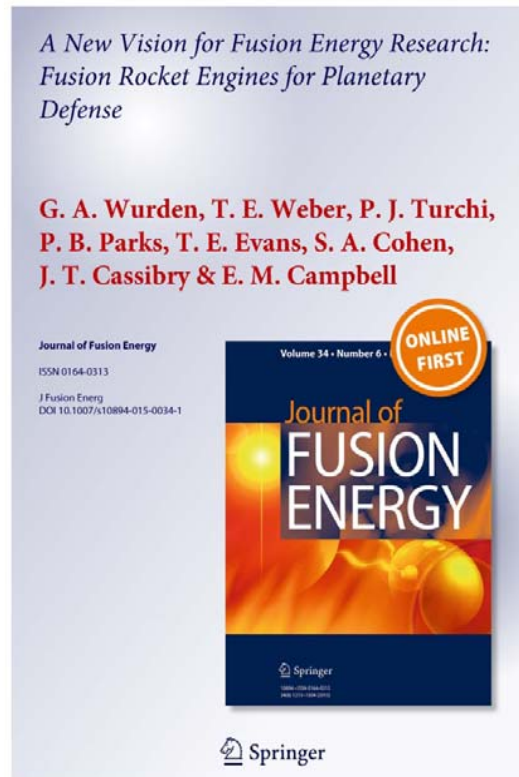
Research Details

Journal of Fusion Energy (Vol 34, No. 6, Nov. 2015).

2015 TEDxLANL by Glen Wurden: [Why did the Dinosaurs need Fusion Rockets too?](#)

A video clip can be found on YouTube.

A fusion rocket workshop is being planned for spring 2016, at PPPL.



J Fusion Energ
DOI 10.1007/s10894-015-0034-1



ORIGINAL RESEARCH

A New Vision for Fusion Energy Research: Fusion Rocket Engines for Planetary Defense

G. A. Wurden¹ · T. E. Weber¹ · P. J. Turchi² · P. B. Parks³ · T. E. Evans⁴ · S. A. Cohen⁵ · J. T. Cassibry⁶ · E. M. Campbell⁶

© The Author(s) 2015. This article is published with open access at Springerlink.com

Abstract We argue that it is essential for the fusion energy program to identify an imagination-capturing critical mission by developing a unique product which could command the marketplace. We lay out the logic that this product is a fusion rocket engine, to enable a rapid response capable of deflecting an incoming comet, to prevent its impact on the planet Earth, in defense of our population, infrastructure, and civilization. As a side benefit, deep space solar system exploration, with greater speed and orders-of-magnitude greater payload mass would also be possible.

Keywords Fusion research · Fusion rocket engine · Comet deflection · Planetary defense · Nuclear explosive

The US Department of Energy's magnetic fusion research program, based in its Office of Science, focuses on plasma and fusion science [1] to support the long term goal of environmentally friendly, socially acceptable, and economically viable electricity production from fusion reactors [2]. For several decades the US magnetic fusion program has had to deal with a lack of urgency towards and inconsistent funding for this ambitious goal. In many American circles, fusion isn't even at the table [3] when it

comes to discussing future energy production. Is there another, more urgent, unique, and even more important application for fusion?

Fusion's Unique Application

As an on-board power source and thruster for fast propulsion in space [4], a fusion reactor would provide unparalleled performance (high specific impulse and high specific power) for a spacecraft. To begin this discussion, we need some rocket terminology. Specific impulse is defined as $I_{sp} = v_e/g$, where g is the usual Earth's gravitational acceleration constant and v_e is the rocket propellant's exhaust velocity. The rocket equation, $M_e/M_i = \exp(-\Delta V/v_e)$, allows us to relate the final mass M_e of the rocket divided by its initial mass M_i , to the change in velocity ΔV that it is capable of achieving. The rocket requires a power source with an output power $P = \alpha M_e$, where we define α to be the specific power (W/kg), and M_e as the mass of the power supply (including the power conditioning, structures, and any waste heat radiators).

Today's best chemical rockets produce propellant exhaust velocities (v_e) up to 4.5 km/s. Fission (nuclear thermal) rocket engines [5] could roughly double that, to about 8.5 km/s (< 5 eV/amu temperature equivalent), constrained by material limits [6]. Electrically driven thrusters [7] are already quite efficient and have higher propellant exhaust velocities (corresponding to ~ 5 eV/amu) but are usually limited in power resulting in low thrust, and are driven by limited electrical power/energy sources (photovoltaic or radioisotope). Development of high power, high thrust plasma thrusters has not been a

✉ G. A. Wurden
wurden@lanl.gov

¹ Los Alamos National Laboratory, Los Alamos, NM, USA

² Santa Fe, NM, USA

³ General Atomics, San Diego, CA, USA

⁴ Princeton Plasma Physics Laboratory, Princeton, NJ, USA

⁵ University of Alabama, Huntsville, Huntsville, AL, USA

⁶ Sandia National Laboratory, Albuquerque, NM, USA

Published online: 16 November 2015

Springer